Catalysis Today 147S (2009) S285–S289

Contents lists available at ScienceDirect

Catalysis Today

journal homepage: www.elsevier.com/locate/cattod

Effect of V_2O_5 additive on simultaneous SO_2 and NO removal from flue gas over a monolithic cordierite-based CuO/Al_2O_3 catalyst

Qingya Liu, Zhenyu Liu *, Weize Wu

State Key Laboratory of Chemical Resource Engineering, Beijing University of Chemical Technology, Beijing, 100029, PR China

ARTICLE INFO

Article history:
Available online 31 July 2009

Keywords:
Monolithic cordierite
CuO/Al_2O_3
Flue gas
V_2O_5 additive
SO_2 removal
SCR

ABSTRACT

A monolithic cordierite-based CuO/Al_2O_3 catalyst showed industrial potential for simultaneous SO_2 and NO removal from flue gases at 350–400 °C. However, it is still a challenge to prevent CuO from aggregation and to keep it in an active state during the removal and regeneration processes. This work shows that addition of V_2O_5 to the catalyst can significantly reduce CuO particle size and improve SO_2 removal activity, and maintain a high selective catalytic reduction (SCR) activity for NO removal. Furthermore, V_2O_5 additive prevents aggregation of SiO_2 in the cordierite with the coated Al_2O_3, and inhibits over reduction of the SO_2 removal product, $CuSO_4$, during the regeneration by NH_3, which are important to the catalyst's stability. V_2O_5 additive changes the regeneration product from Cu_3N to CuO and thus may avoid the temperature rise and NOx release in the subsequent removal process.

1. Introduction

Monoliths are increasingly being used as catalyst supports in many new reactor applications, such as chemical process, refining industries, catalytic combustion, due to advantages over conventional packed bed reactors (easy to handle, low pressure drop, attrition-free, etc.) [1]. Recently, we formulated a monolithic cordierite-based CuO/Al_2O_3 catalyst for simultaneous SO_2 and NO removal from flue gas [2], which combines the high activities of CuO/Al_2O_3 at 300–400 °C [3] and the low flow resistance and high mechanical strength of monolithic cordierite. Na_2O additive was introduced to the formulation to increase SO_2 capture capacity, but it significantly inhibited selective catalytic reduction (SCR) of NO by NH_3 due to increased NH_3 over reduction [4]. Therefore, an additive, which can improve CuO dispersion but do not poison the SCR reaction, is required to advance the formulation.

V_2O_5 is believed to be a desired alternative to Na_2O because it has been demonstrated to be able to improve CuO dispersion on AC [5] and Al_2O_3 [6] and used widely as a catalytic component of TiO_2-, carbon- and Al_2O_3-based catalysts for SCR of NO with NH_3 [7,8]. In this work, the detailed studies have been performed on the effects of V_2O_5 additive on properties and activities of monolithic cordierite-based CuO/Al_2O_3 with the aid of X-ray powder diffraction (XRD), scanning electron microscopy (SEM), extended X-ray adsorption fine structure (EXAFS) and X-ray photoelectron spectroscopy (XPS).

2. Experimental

2.1. Catalyst preparation

The cordierite used is a commercial product with a cell density of 200 cells per square inch (cpsi) and a BET surface area of 0.7 m^2/g. The catalysts preparation includes an acid treatment of the cordierite, coating of γ-Al_2O_3 and impregnation of V_2O_5 and then CuO. The acid treatment was performed with 50 wt.% oxalic acid as described in our earlier work [2]. Al_2O_3 was coated on the treated cordierite using a sol synthesized from urea and alumina nitrate. The samples were immersed into the sol for 6 h, then removed for drying at 110 °C overnight and calcining at 500 °C for 8 h. This coating process was repeated for 5 times to obtain an Al_2O_3 loading of about 20%. The Al_2O_3-coated cordierites were then immersed into an aqueous solution of ammonium metavanadate in oxalic acid. After drying, CuO was loaded using an aqueous solution of copper nitrate, followed by drying and calcining. The resulting catalysts are named according to the loadings of V and Cu. For example, V0.5Cu7 refers to a catalyst with 0.5 wt.% V and 7.0 wt.% Cu. To facilitate discussion, short names are given to the catalysts at different stages, where F in a bracket represents the fresh catalyst, S represents the sulfated catalyst (subjected to simultaneous SO_2 and NO removal), and R represents the catalyst regenerated as described in Section 2.3. For comparison, Na_2O doped catalysts are termed Cu7NaX, where X denotes sodium loading.

---

* Corresponding author. Tel.: +86 10 64421073; fax: +86 10 64421073.
E-mail address: liuzy@mail.buct.edu.cn (Z. Liu).

0920-5861/$ – see front matter © 2009 Elsevier B.V. All rights reserved.
doi:10.1016/j.cattod.2009.07.013

2.2. Characterization of the catalysts

SEM photographs were obtained on a JEOL JSM-35C scanning microscope. Prior to SEM analysis, the samples were embedded in epoxy resin, metallographically polished and coated with a conductive layer of gold.

XRD was performed on a Riguku D/Max 2500 system. Diffraction patterns were recorded with Cu Kα (λ = 0.1542 nm) radiation and the X-ray tube was operated at 40 kV and 100 mA. The step scans were taken in the range of 2θ from 10° to 80° at a speed of 8°/min.

EXAFS was used to determine the chemical forms of Cu species in the catalysts. The measurements were performed on wiggler beam line 4W1B at Beijing Synchrotron Radiation Facility (BSRF). A double crystal of Si (1 1 1) was used to monochromatize X-rays from a 2.2 GeV electron storage ring with an average ring current of 80 mA. Cu K-edge absorption spectra were recorded in transmission mode. Fourier transformation was performed on the k^3 weighted EXAFS oscillation.

XPS measurements were carried out at room temperature on a VG Scientific ESCA-Lab 220I-XL spectrometer with Al-Kα radiation in twin anode ($h\nu$ = 1486.6 eV) at 10 kV × 20 mA. The binding energies were corrected by the C1s peak at 284.6 eV. XPS data analysis was performed with the XPS-Peak3.1 program and the spectra were fitted with an optimal Gaussian–Lorentzian ratio after subtraction of a Shirley-type baseline.

2.3. Activity test

The activity test was carried out in a fixed-bed reactor of 22 mm in diameter. At steady state of 400 °C, a gas mixture containing 1960 ppm SO_2, 500 ppm NO, 5.5% O_2, 2.5% H_2O, 500 ppm NH_3 and balance Ar was introduced into the reactor. The total flow rate was controlled at 440 ml/min, corresponding to a superficial space velocity of 2800 h^{-1}. When SO_2 conversion decreased to about 70%, the catalyst was regenerated in situ in 5% NH_3/Ar (300 ml/min) at 400 °C for 1.5 h and purged with Ar for 1 h. Then, the above gas mixture was introduced into the reactor for the second reaction cycle. The concentrations of NO, SO_2 and O_2 in the inlet and outlet of the reactor were simultaneously monitored on-line by a Flue Gas Analyzer (KM9106, Kane, Germany).

3. Results and discussion

3.1. Effect of V_2O_5 on the physico-chemical properties of the fresh catalyst

Taking V1.1Cu7(F) as an example, the effect of V_2O_5 on the physico-chemical properties of the catalyst is studied by SEM and XRD. Fig. 1 shows SEM images of Cu7(F) and V1.1Cu7(F). Cu7(F) has been discussed in detail in our previous work [4]. It was confirmed that the cotton-like conglomerations with sizes ranging from 13 to 20 μm resulted from interaction of SiO_2 in the cordierite with the

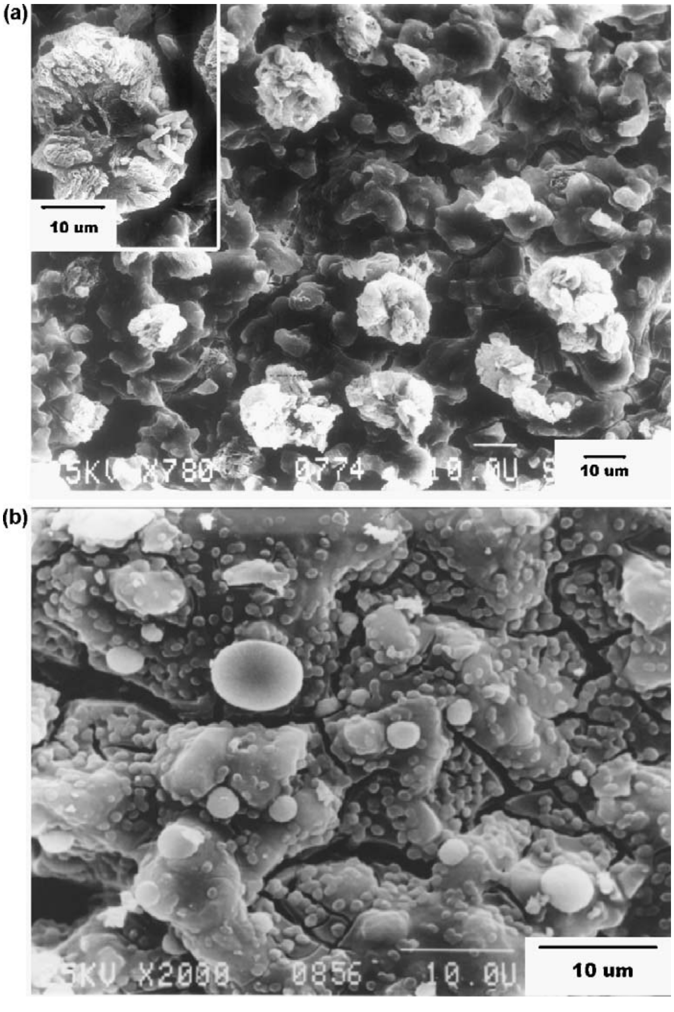

Fig. 1. SEM images of (a) Cu7(F) sample (×780) and (b) V1.1Cu7(F) sample (×2000).

coated Al_2O_3 during loading CuO. The rods with length of about 3 μm surrounded by the cotton-like conglomerations (see the enlarged image at the top left corner) were confirmed to be well-crystallized CuO. SEM image of V1.1Cu7(F) is clearly different from that of Cu7(F). Small global particles with sizes of about 1 μm are uniformly distributed on V1.1Cu7(F) surface, along with fewer larger particles with sizes of about 3 μm. Particles of about 6–8 μm can also be observed, but very few. The absence of cotton-like conglomerations on V1.1Cu7(F), compared to Cu7(F), indicates that V_2O_5 additive prevents aggregation of SiO_2 in the cordierite with the coated Al_2O_3. This may be related to the loading sequence of active components, V_2O_5 first and then CuO, since the aggregation is initiated by CuO [4]. Doping V_2O_5 before CuO loading may form a vanadium film, which inhibits the initiation behavior of CuO.

EDX analysis indicates that the particles of about 3 μm in diameter on V1.1Cu7(F) contains Cu, O and less V, and the particles of about 1 μm in diameter contains Al, Si, O and Cu. It should be pointed out that Al and Si detected in the particles of about 1 μm are possibly from the cordierite and Al_2O_3 because the detection depth of EDX, 2–3 μm, is beyond the particle size. To elucidate the specific forms of the particles on V1.1Cu7(F), Fig. 2 shows the XRD results. Compared to XRD pattern of Al_2O_3-coated cordierite, Cu7(F) shows new peaks at 35.6° and 38.8°, indicating the presence of CuO crystal ($2\theta = 35.6°$ and 38.8°). When V_2O_5 is added to Cu7(F), the diffraction peaks of CuO still exist (see V1.1Cu7(F)), but their intensities become weaker. This suggests that all the particles on V1.1Cu7(F) observed by SEM are CuO and V_2O_5 additive may greatly improve CuO distribution on the γ-Al_2O_3-coated cordierite (most of CuO particles are reduced from about 3 μm to about 1 μm in diameter). Furthermore, diffraction peaks of V_2O_5 ($2\theta = 20.4°$, 25.8° and 31.0°) or other forms of vanadium cannot be observed, which suggests that vanadium species is well dispersed or in amorphous form.

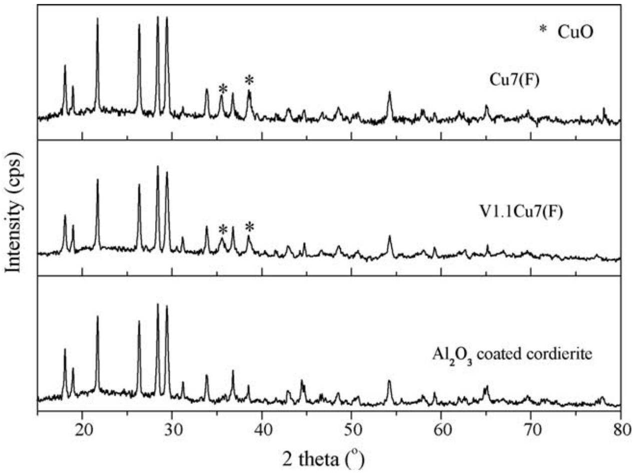

Fig. 2. XRD patterns of the different catalysts and Al_2O_3-coated cordierite.

3.2. Effect of V_2O_5 on SO_2 and NO removal activities

3.2.1. SO_2 removal activity

Fig. 3a shows SO_2 conversions versus time over the catalysts with different V_2O_5 loading, along with sulfur capacity (termed SC_{80}). SC_{80} is defined as the amount of SO_2 adsorbed on the catalyst, in wt.%, during the time frame of SO_2 conversions of not less than 80%. In the first reaction cycle (for the fresh catalysts), SC_{80} increases from 2.3 to 5.5 wt.% with increasing vanadium loading from 0 to 1.6 wt.%, but decreases to 3.2 wt.% with further increasing vanadium loading to 2.1 wt.%. Clearly, V_2O_5 significantly increase SO_2 removal activity, which can be attributed to the improved CuO dispersion.

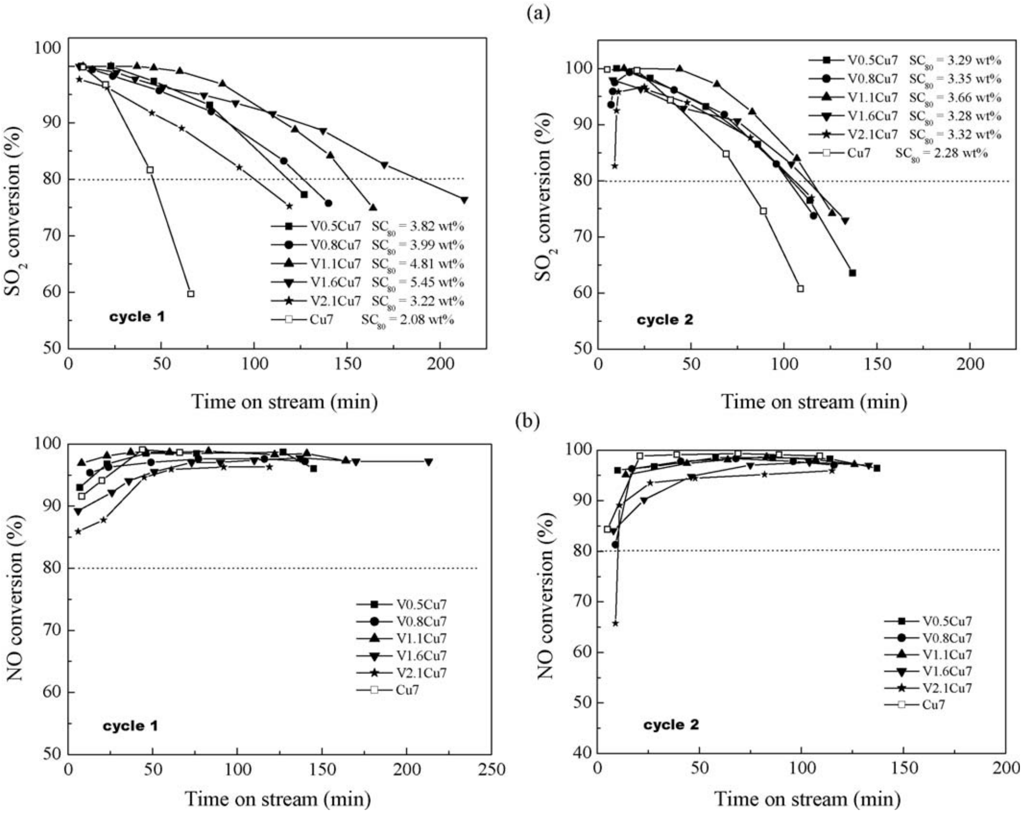

Fig. 3. Effect of V_2O_5 loading on (a) SO_2 removal activity and (b) SCR activity.

In the second reaction cycle (for the regenerated catalysts), the presence of V_2O_5 in the catalyst also improves SO_2 removal activity and SC_{80} increases from 2.3 wt.% for Cu7 to 3.3–3.7 wt.% for V_2O_5 doped catalysts. Obviously, the improvements of V_2O_5 in the second reaction cycle are not as high as those in the first reaction cycle, suggesting that the sulfur captured by the catalysts in the first reaction cycle cannot be removed thoroughly during the regeneration. Even so, the SC_{80} is enhanced by 43% when 0.5 wt.% V_2O_5 is added to the catalyst, which means that the regeneration frequency can be reduced by half. A vanadium loading of 0.5% is more advisable for better economy, since SC_{80} increases only slightly from 3.3 to 3.7 wt.% with increasing V_2O_5 loading from 0.5 to 1.1 wt.%.

3.2.2. SCR activities

Fig. 3b presents the effect of V_2O_5 loading on the SCR activities. For all the catalysts in the two cycles, NO conversion increases with time until to a steady state. This phenomenon, as observed on CuO/Al_2O_3 catalysts, is attributed to the formation of sulfates during the reaction, which increases NH_3 adsorption and inhibits over-oxidation (or activation) of NH_3 [9]. Steady state NO conversions of all the catalysts in the two cycles are above 95%, which is far higher than those of Cu7NaX catalysts reported earlier [4], 85% or below. This suggests that V_2O_5 additive, unlike Na_2O additive, has no inhibition effect on the SCR reaction of NO with NH_3 and maintains the high SCR activity of the cordierite-based CuO/Al_2O_3.

To obtain high SO_2 and NO removal activities simultaneously and for better economy, the catalyst with a vanadium loading of 0.5 wt.% is recommended.

3.3. Effect of V_2O_5 on the solid regeneration products

It was interesting to point out that for Cu7 and Cu7NaX catalysts, an obvious temperature rise of about 15 °C was observed in the first 5 min of the second removal cycle. However, for the catalysts with V_2O_5 as an additive, the temperature rise almost cannot be observed. This suggests that V_2O_5 additive influences the forms of copper in the regenerated catalysts.

Our previous work [4,10] has shown that Cu_3N was the regeneration product of the sulfated Cu7NaX and CuO/Al_2O_3. Cu_3N is oxidized by O_2 to form CuO in the second reaction cycle, which results in large heat release and thus an obvious temperature rise. This behavior unfavors to the catalyst stability and may cause many operation problems in industrial application. To confirm the regeneration product of the catalysts with V_2O_5 as an additive, XRD, EXAFS and XPS were performed on V1.1Cu7.

Fig. 4 exhibits XRD pattern of V1.1Cu7(R), along with those of Cu7(R) and Al_2O_3-coated cordierite for comparison. It is clear that strong diffraction peaks of Cu_3N (23.2°, 40.9° and 47.6°) can be observed for Cu7(R). When V_2O_5 additive is used, the diffraction peaks of Cu_3N disappear (see V1.1Cu7(R)). In addition, the XRD pattern and intensity of V1.1Cu7(R) are similar to those of Al_2O_3-coated cordierite, and no copper species can be detected by XRD. These results suggest that the solid regeneration product in V1.1Cu7(R) is well dispersed.

To further determine the form of copper species on V1.1Cu7(R), EXAFS and XPS analysis were used. Fig. 5 shows the radial structure function (RSF) spectrum of V1.1Cu7(R) obtained by EXAFS characterization, along with that of Cu7Na2(R) for comparison. It should be pointed out that the RSF is not corrected for phase shift. Cu7Na2(R) has been discussed in our previous work [4], where the two strong peaks at 1.45 and 2.31 Å were confirmed to be the typical signals of Cu_3N (1.45 Å for Cu–N bond and 2.31 Å for Cu–Cu bond). For V1.1Cu7(R), the absence of peak at 2.31 Å indicates that its copper species is not in the form of Cu_3N, and the strong peak at 1.50 Å and the weak peak at 2.43 Å suggest that its copper species is mainly in the form of CuO (1.5 Å for Cu–O bond and 2.5 Å for Cu–Cu bond [11,12]). An additional shoulder peak at 2.02 Å can also be observed on V1.1Cu7(R), which is possibly due to the presence of metal Cu (1.9–2.2 Å for Cu–Cu bond [13]).

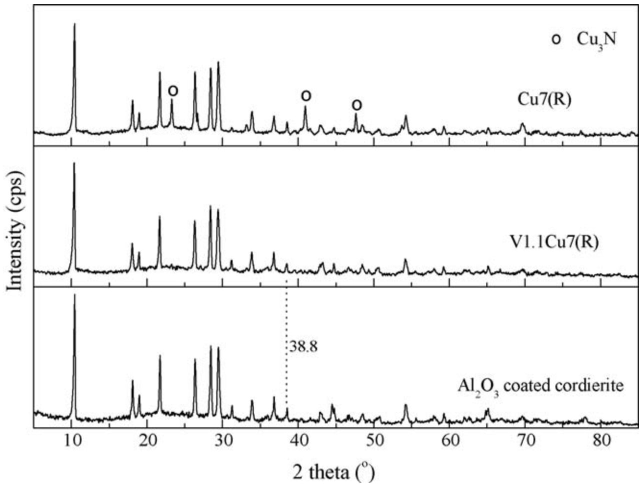

Fig. 4. XRD patterns of the regenerated catalysts and Al_2O_3-coated cordierites.

Fig. 6 shows XPS spectra of Cu 2p of V1.1Cu7 at different stages. All the samples present the main and satellite peaks of Cu $2p_{3/2}$ (930–938 eV and 940–948 eV, respectively) and the main and satellite peaks of Cu $2p_{1/2}$ ((950–958 eV and 960–965 eV, respectively). As usual, only the peaks of Cu $2p_{3/2}$ are fitted and discussed. Gaussian–Lorentzian fit to Cu $2p_{3/2}$ of V1.1Cu7(F) indicates that its main peak is composed of two peaks at 933.9 and 935.5 eV (Fig. 6A). The former is assigned to Cu^{2+} in CuO [14,15] and the latter is tentatively assigned to Cu^{2+} in $CuAl_2O_4$ according to the literature [16]. The main peak of Cu $2p_{3/2}$ of V1.1Cu7(S) is fitted satisfactorily to three principal peaks at 933.1, 935.6 and 937.5 eV (Fig. 6B). The peak at 935.6 eV is assigned to $CuSO_4$ according to the literatures [14,17], which is confirmed by the split satellite peaks at 940.8 and 944.2 eV. The peak at 937.5 eV is assigned to Cu^{2+} in the sulfated $CuAl_2O_4$ by analyzing the spectra of S 2p and Al 2p (not shown in this work). Gaussian–Lorentzian fit to Cu $2p_{3/2}$ of V1.1Cu7(R) indicates that its main peak is composed of two peaks at 933.0 and 935.2 eV (Fig. 6C). Combined with S 2p spectrum of V1.1Cu7(R) (not shown in this work), the peak at 935.2 eV is found to be Cu^{2+} in $CuSO_4$. That is to say, a part of $CuSO_4$ formed during reaction cannot be regenerated by NH_3, which is

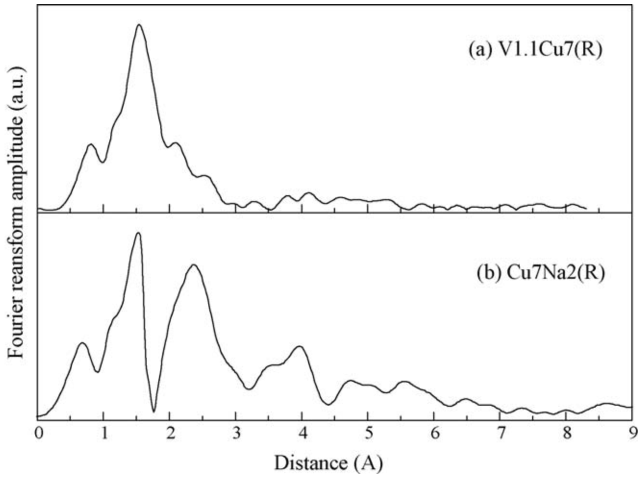

Fig. 5. The Cu K-edge EXAFS RSFs of (a) V1.1Cu7(R) and (b) Cu7Na2(R).

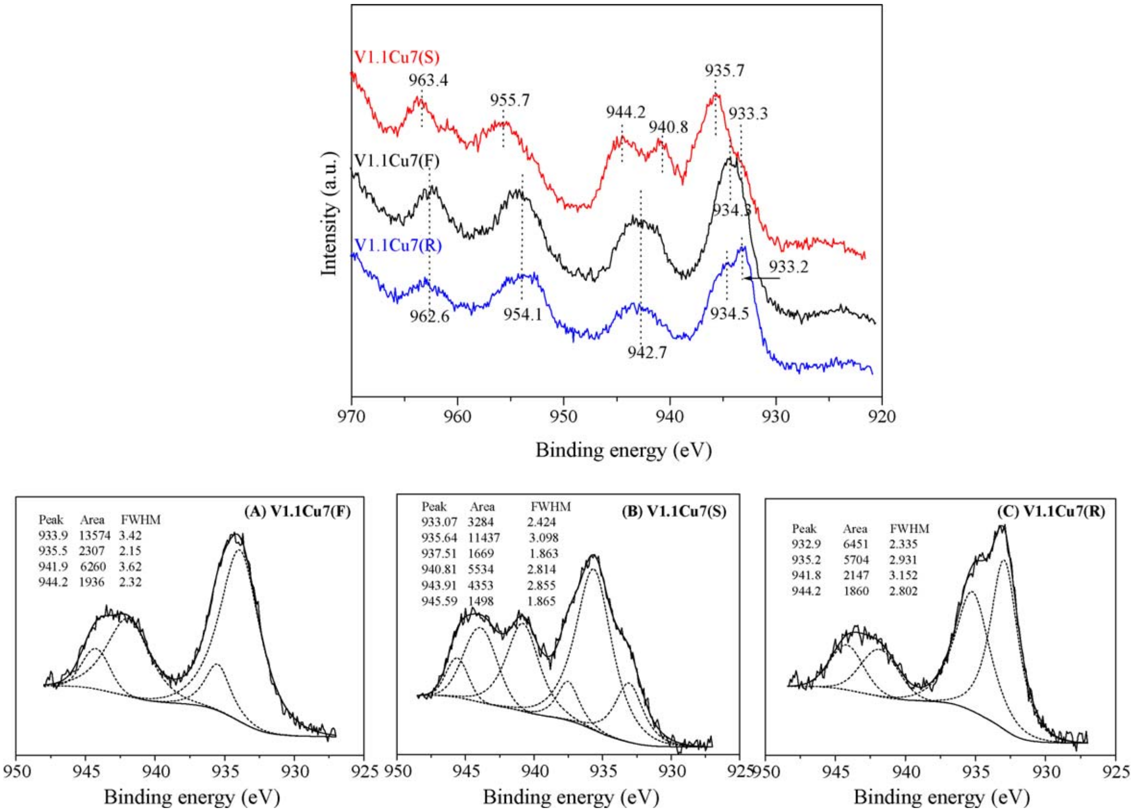

Fig. 6. XPS spectra of Cu 2p in V1.1Cu7 catalysts at different stages.

consistent with the activity test result that SC_{80} of the regenerated catalysts are lower than those of the fresh catalysts. The peak at 933.0 eV observed on V1.1Cu7(S) and V1.1Cu7(R) is attributed to Cu^{2+} $2p_{3/2}$ in CuO, but not to Cu or Cu^{+}, due to the presence of strong satellite peak at 940–948 eV (note: the satellite peak is usually used as a characteristic to determine Cu^{2+}). It is not surprise that the binding energy of Cu^{2+} in V1.1Cu7(F) is located at 933.9 eV, while that in V1.1Cu7(R) is located at 933.0 eV, since the intensity and location of XPS peak depends on both ion density and its chemical environment [18].

The data presented so far confirm that the regeneration product of V1.1Cu7(S) by NH_3 is mainly well-dispersed CuO, not Cu_3N as observed on Cu7 and Cu7NaX catalysts. That is to say, V_2O_5 additive inhibits over reduction of $CuSO_4$ by NH_3 to Cu_3N, which is important because of avoidance of the temperature rise and NO release in the subsequent removal cycle. It is also important to the catalyst's stability.

4. Conclusions

Addition of V_2O_5 to the monolithic cordierite-based CuO/Al_2O_3 catalyst has great influences on its properties. V_2O_5 significantly improves CuO distribution and thus SO_2 removal capacity. A vanadium loading of 0.5 wt.% is sufficient to yield a catalyst with a high SO_2 removal activity. V_2O_5 additive, compared to Na_2O additive used in our previous works, does not poison the SCR reaction of NO by NH_3 and maintains a high SCR activity of the cordierite-based CuO/Al_2O_3 catalyst. More importantly, V_2O_5 additive prevents aggregation SiO_2 in the cordierite with the coated Al_2O_3 initiated by CuO and inhibits over reduction of $CuSO_4$ by NH_3 in the regeneration process, which is an important finding not only for stability of the catalyst in this work but also for formulation of other catalyst. V_2O_5 additive changes the regeneration product from Cu_3N for the cordierite-based CuO/Al_2O_3 to CuO, which may avoid the temperature rise and NOx release in the subsequent removal process.

Acknowledgements

The authors gratefully acknowledge the Natural Science Foundation of China (20606002, 20736001 and 20821004) for financial supports.

References

[1] J.L. Williams, Catal. Today 69 (2001) 3.
[2] Q. Liu, Z. Liu, Z. Huang, G. Xie, Catal. Today 93–95 (2004) 833.
[3] C. Macken, B.K. Hodnett, G. Paparatto, Ind. Eng. Chem. Res. 39 (2000) 3868.
[4] Q. Liu, Z. Liu, G. Xie, Z. Huang, Ind. Eng. Chem. Res. 43 (2004) 4031.
[5] S.A.C. Carabineiro, A.M. Ramos, J. Vital, J.M. Loureiro, J.J.M. Órfão, I.M. Fonseca, Catal. Today 78 (2003) 203.
[6] R. Wang, T. Chen, G. Zhang, C. Hu, A. Tian, Nat. Gas Chem. (Chin. J.) 24 (1999) 12.
[7] P. Forzatti, Appl. Catal. A 222 (2001) 221.
[8] Z. Huang, Z. Zhu, Z. Liu, Appl. Catal. B 39 (2002) 361.
[9] G. Xie, Z. Liu, Z. Zhu, Q. Liu, J. Ge, Z. Huang, J. Catal. 224 (2004) 42.
[10] G. Xie, Z. Liu, Z. Zhu, Q. Liu, J. Ma, Appl. Catal. B 45 (2003) 213.
[11] D. Chen, Z. Wu, Radiat. Phys. Chem. 75 (2006) 1921.
[12] K. Fukumi, A. Chayahara, K. Kadono, H. Kageyama, T. Akai, N. Kitamura, M. Makihara, K. Fujii, J. Hayakawa, J. Non-Cryst. Solids 238 (1998) 143.
[13] E.A. Stern, D.E. Sayers, F.W. Lytle, Phys. Rev. B 11 (1975) 4836.
[14] B.R. Strohmeier, D.E. Levden, R. Scott Field, D.M. Hercules, J. Catal. 94 (1985) 514.
[15] J. Zhou, Q.H. Xia, S.C. Shen, S. Kawi, K. Hidajat, J. Catal. 225 (2004) 128.
[16] F. Severino, J.L. Brito, J. Laine, J.L.G. Fierro, A. López Agudo, J. Catal. 177 (1998) 82.
[17] V.I. Nefedov, E.K. Zhumadilov, T.Yu. Konitova, J. Struct. Chem. USSR 18 (1977) 549.
[18] V.I. Nefedov, X-ray Photoelectron Spectroscopy of Solid Surfaces, Brill Academic Publishers, 1988.